THE ANNALS OF “DUNĂREA DE JOS” UNIVERSITY OF GALAȚI
FASCICLE V, TECHNOLOGIES IN MACHINE BUILDING,
ISSN 1221- 4566, 2012

GLOBAL AND LOCAL STRENGTH ASSESSMENT, UNDER EQUIVALENT QUASI-STATIC HEAD WAVE LOADS, BASED ON THREE CARGO HOLD 3D-FEM MODEL, OF AN 1100 TEU CONTAINER SHIP

Ionica Rubanenco, Iulia Mirciu, Leonard Domnisoru

“Dunarea de Jos” University of Galati, Naval Architecture Faculty, Romanian
ionicaru@yahoo.com

ABSTRACT

In this paper is presented the global-local strength numerical analysis for an 1100 TEU container ship. The numerical analysis is carried on 3D-CAD/FEM model using SolidWorks Cosmos/M software. The model has three cargos holds and is analysed for two loading cases: full and intermediary (no containers on deck). The considered loads are: own-weight, containers weight, still water and equivalent quasi-static head wave loads, according to the Germanischer Lloyd Rules. The numerical analysis emphasizes the hot spot stresses on the three cargos holds model, making possible to obtain the hot spot factors used for the correlation between 1D-3D structure modelling.

KEYWORDS: global-local strength analysis, container ship, 3D-CAD/FEM model

1. INTRODUCTION

In order to increase the accuracy of ship structures assessment, it is required to carry out a strength analysis based on 3D-CAD/FEM models, according to Frieze & Shenoi [5], Lehmann [6], Domnisoru [2].

This paper is focused on the global-local strength analysis of an 1100 TEU container ship, based on three cargo holds 3D-CAD/FEM models. There are considered two loading cases: full cargo, with containers in the cargo holds and on deck, and intermediary condition, without containers on the deck. As external load is considered the equivalent quasi-static head wave, modelled according to the Germanischer Lloyd Rules [4].

2. 1100 TEU CONTAINER SHIP MAIN CHARACTERISTICS

The analysed ship is a general cargo container ship, with five cargo holds and two hatch rows. The cargo holds number one, two and five are provided with two decks and the cargos holds number three and four have one deck.

The ship has three deck cranes with a maximum lifting capacity of 30 tonnes each. Table 1 presents the main dimensions and form coefficients of the ship. The distance between ordinary frames a_0 and strengthened frames a_{Fr}, W_{DL}, W_B, the vertical bending modules and other data are presented in Table 1.

The external equivalent quasi-static head wave height h_w is considered according to the Germanischer Lloyd Rules [4].

Table 1. *1100 TEU container ship main characteristics*

L_{max} [m]	173.42	a_{Fr} [mm]	3200
L_{pp} [m]	164	Δ [t]	29673
B_{max} [m]	27.3	ρ [t/m^3]	1.025
D_{max} [m]	14.6	W_{DL} [m^3]	10.530
T_{full} [m]	8.5	W_B [m^3]	15.448
v [knots]	18	c_B	0.758
Crew [per.]	25	deadweight [t]	22200
TEU	1100	$h_{w\,GL}$ [m]	9.326
a_0 [mm]	800	$x_{G\ full}$ [m]	88.3

Fig. 1 presents the general arrangement of the ship and the selected three cargo holds for the strengths analysis. The analysed three cargo holds are positioned amidships (numbers four, three and half of cargo hold two) as presented in Fig.1, marked with a border.

The general arrangement presents the position and the number of the containers on the ship deck and also the position and number of containers from the cargos holds.

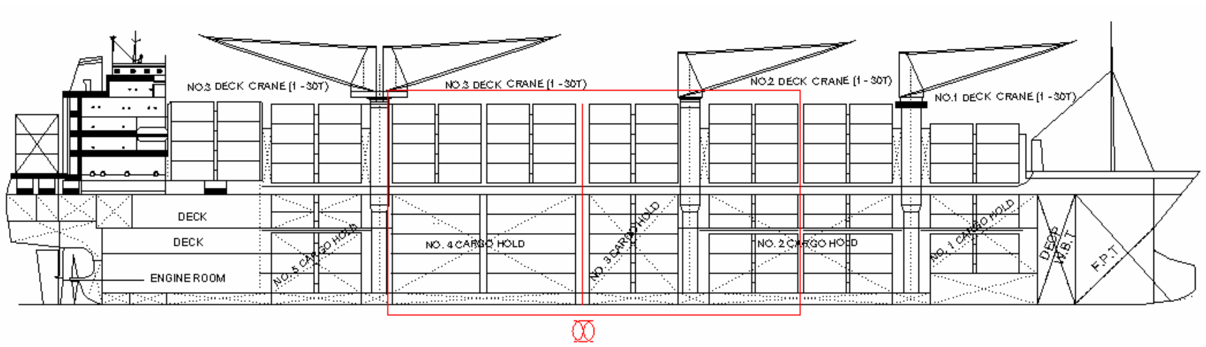

Fig. 1. *General arrangement of the 1100 TEU container ship*

3. 3D-FEM MODEL DESCRIPTION

The analysed model is developed for three cargo holds in compliance with the Germanischer Lloyd Rules [4], for the cargos holds 4, 3 and 2 (1/2).

Table 2 presents the material characteristics and the minimum yielding stress required by the rules [4].

Table 2. *Ship material characteristics*

E [N/mm^2]	2.1E+05	$\tau_{adm-AH36}$ [N/mm^2]	153
ρ_{mat} [t/m^3]	7.7	R_{eH-A} [N/mm^2]	235
$R_{eH-AH36}$ [N/mm^2]	355	σ_{adm-A} [N/mm^2]	175
$\sigma_{adm-AH36}$ [N/mm^2]	243	τ_{adm-A} [N/mm^2]	110

Table 3 describes the component elements of 3D-CAD/FEM model and the master nodes from aft and fore part of model used for applying the boundary conditions and the global bending moment.

Table 3. *Three cargo holds 3D-FEM model characteristics*

Number of nodes	ND_{max}	85916
Number of shell3T elements	EL_{max}	207463
Number of element groups	EG	296
Support condition aft node	ND_{aft}	85585
Support condition fore node	ND_{fore}	85586

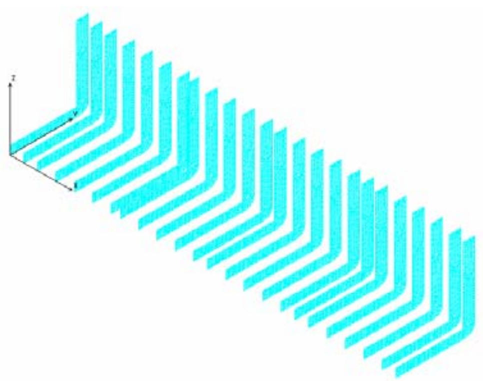

Fig. 2. *Strengthened frames along the 3D-FEM model*

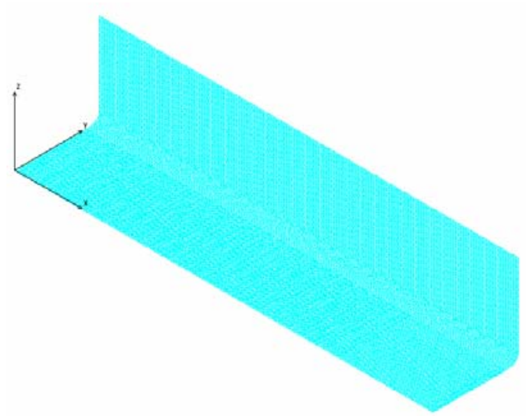

Fig. 3. *Shell elements from bottom and side plates*

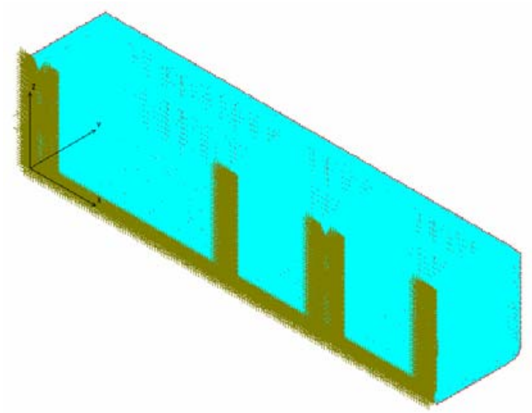

Fig. 4. *Boundary conditions on 3D-FEM model*

Fig. 2 presents the strengthened frames and Fig. 3 presents shell elements from the side and bottom plates for the three cargos holds 3D-FEM model.

The boundary conditions are of two types:

1) the centre line nodes ship symmetry condition, because the model is developed on only just one side;

2) at the model both ends are considered two-nodes of rigid solid element type, between the aft and fore model nodes (Table 3), disposed at the neutral axis, and the selected nodes from aft-fore model nodes of the longitudinal structural elements. In the support nodes from aft-fore model are applied the global bending moments resulting from a 1D-FEM analysis.

4. THE THREE CARGO HOLDS MODEL STRENGTH ANALYSIS

4.1. Full cargo case

In the following tables are included the next numerical results:

- the floating and trim in vertical plan equilibrium parameters, h_w, d_{aft}, d_{fore} , d_m, trim, for sagging and hogging cases (Table 4), full cargo case;
- the maximum normal stress $\sigma_{x\text{-max}}$ [N/mm^2] using 3D-CAD/FEM and 1D-FEM models at sagging and hogging loading cases and their ratio, for deck RL and bottom (Table 5 and 6), in case of full cargo;
- the maximum tangential stress in the neutral axis, $\tau_{xz\text{-max}}$ [N/mm^2] using 3D-CAD/FEM and 1D-FEM models at sagging and hogging loading cases and their ratio (Table 7), in case of full cargo.

Table 4. *The floating and trim in vertical plan equilibrium parameters, full cargo*

h_w [m]	3D FEM Hogging			
	d_{aft}[m]	d_{fore}[m]	d_m[m]	trim [rad]
0	8.502	8.502	8.502	0.00000
5	8.280	7.706	8.003	-0.00331
9.326	7.439	7.386	7.413	-0.00031
12	6.769	7.242	7.000	0.00273
	3D FEM Sagging			
0	8.502	8.502	8.502	0.00000
5	8.329	9.342	8.807	0.00584
9.326	8.208	9.867	8.990	0.00957
12	8.165	10.097	9.077	0.01114

Table 5. *The maximum (max) deck normal stress, full cargo case*

Hogging	$\sigma_{x\text{-max}}$ Deck RL [N/mm^2] z=16m		
h_w [m]	1D	3D-FEM	3D/1D
0	31.88	59.60	1.87
5	35.96	46.09	1.28
9.326	**77.23**	**100.90**	**1.31**
12	100.47	132.40	1.32
adm	224	224	
max_{GL}/adm	0.34	0.45	
Sagging	$\sigma_{x\text{-max}}$ Deck RL [N/mm^2] z=16m		
0	31.88	59.60	1.87
5	104.79	135.2	1.29
9.326	**175.16**	**226.60**	**1.29**
12	221.01	285.90	1.29
adm	224	224	
max_{GL}/adm	0.78	1.01	

Table 6. *The maximum (max) bottom normal stress, full cargo case*

Hogging	$\sigma_{x\text{-max}}$ Bottom [N/mm^2] z=0		
h_w [m]	1D	3D-FEM	3D/1D
0	21.73	73.72	3.39
5	24.51	81.79	3.33
9.326	**52.65**	**119.00**	**2.26**
12	68.49	146.20	2.13
adm	175	175	
max_{GL}/adm	0.30	0.68	
Sagging	$\sigma_{x\text{-max}}$ Bottom [N/mm^2] z=0		
0	21.73	73.72	3.39
5	71.44	182	2.55
9.326	**119.4**	**159.3**	**1.33**
12	150.66	189.4	1.26
adm	175	175	
max_{GL}/adm	0.68	0.91	

Table 7. *The maximum (max) neutral axis tangential stress, full cargo case*

Hogging	$\tau_{xz\text{-max}}$ Neutral axis [N/mm^2]		
hw	1D	3D-FEM	3D/1D
0	29.80	20.45	0.69
5	36.76	19.76	0.54
9.326	**54.01**	**33.04**	**0.61**
12	64.09	41.9	0.65
adm	110	110	
max_{GL}/adm	0.49	0.30	
Sagging	$\tau_{xz\text{-max}}$ Neutral axis [N/mm^2]		
0	29.80	20.45	0.69
5	61.89	22.30	0.36
9.326	**92.01**	**38.76**	**0.42**
12	111.45	49.38	0.44
adm	110	110	
max_{GL}/adm	0.84	0.35	

In the following figures are presented the global-local strength numerical results, in full cargo case:

- Fig.5 presents the mass diagram full cargo;
- the bending moment M [N/mm^2] diagram, based on 1D-girder model, for Deck RL (z=16m) and Bottom (z=0) wave height h_w=0-12m (Fig.6 and 7);
- the neutral axis normal stress τ_{xz} [N/mm^2] diagram, based on 1D-girder model, for wave height h_w=0-12m (Fig.8);

- the bending moment M [N/mm^2] diagram, based on 3D-CAD/FEM model, for Deck RL (z=16m) and Bottom (z=0) wave height h_w=0-12m (Fig.9 and 10);

- the neutral axis normal stress τ_{xz} [N/mm^2] diagram, based on 3D-CAD/FEM model, for wave height h_w=0-12m (Fig.11).

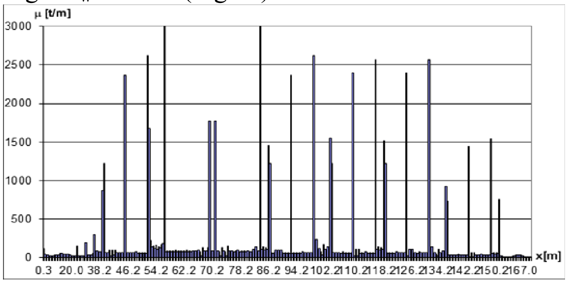

Fig. 5. *Mass distribution full cargo*

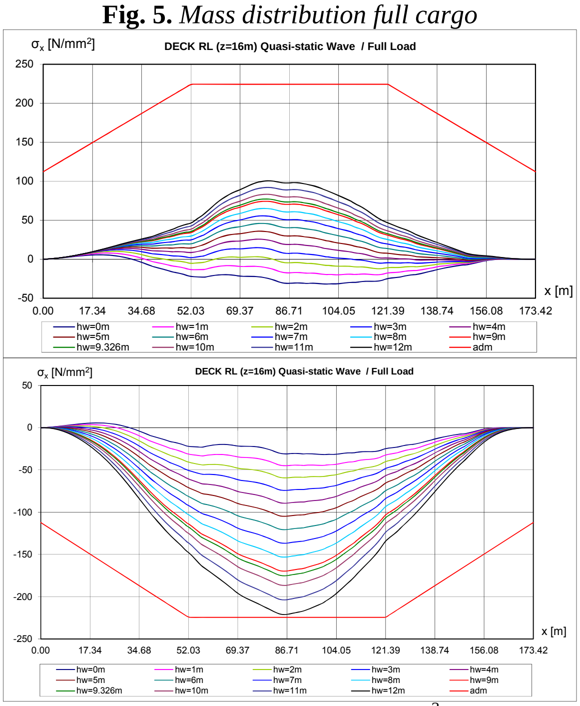

Fig. 6. *Normal stress Deck RL [N/mm^2] 1D hogg, sagg*

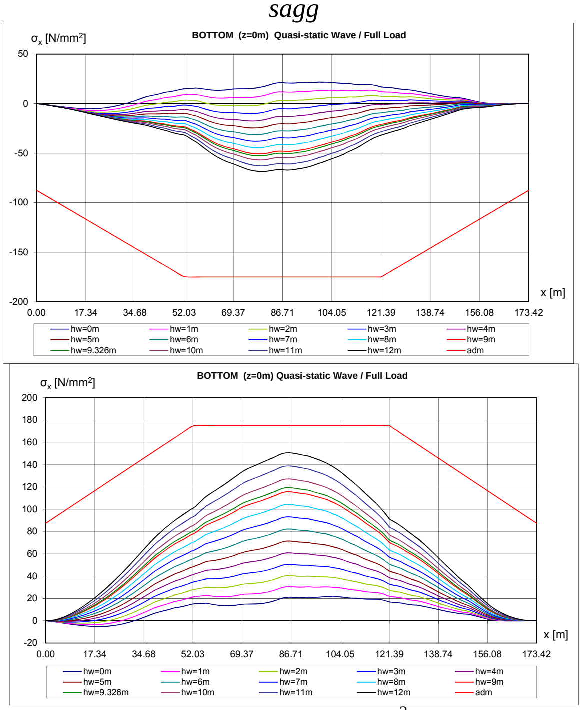

Fig. 7. *Normal stress Bottom [N/mm^2] 1D hogg, sagg*

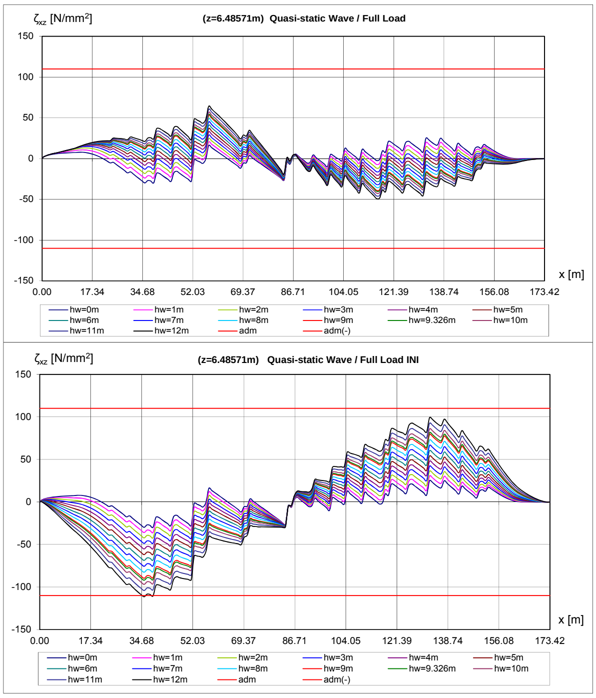

Fig. 8. *Tang.n-n stress [N/mm^2] 1D hogg, sagg*

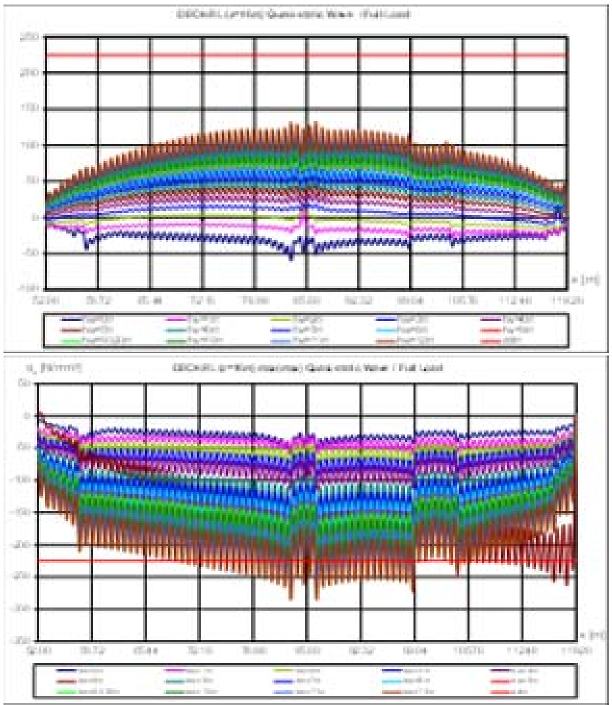

Fig. 9. *Normal stress Deck RL [N/mm^2] 3D hogg, sagg*

In the following figures, are presented the numerical results in case of full cargo:

- the equivalent von Mises stress [N/mm^2] distribution , at wave height h_w=9.326m, based on the 3D-FEM model, hogg and sagg case (Fig.12);
- the equivalent von Mises stress [N/mm^2] distribution for Deck RL (z=16m), Deck (z=14.5m) and Bottom (z=0), at wave height h_w=9.326m, based

on the 3D-FEM model, hogg and sagg case (Fig.13, 14 and 15).

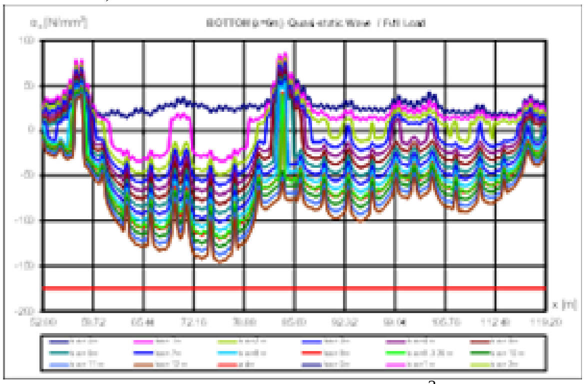

Fig. 10.a. *Normal stress Bottom [N/mm^2] 3D hogging*

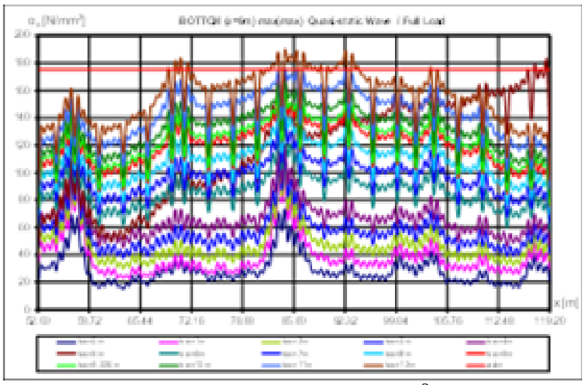

Fig. 10.b. *Normal stress Bottom [N/mm^2] 3D sagging*

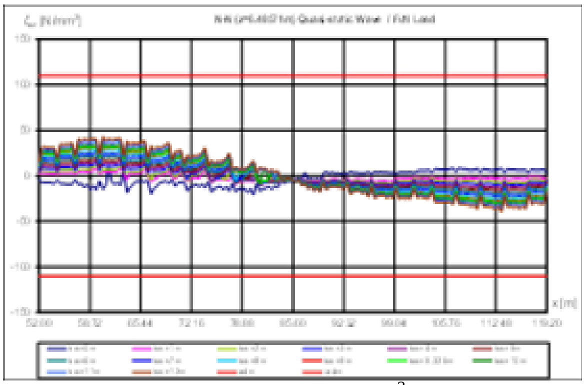

Fig. 11.a. *Tang.n-n stress [N/mm^2] 3D hogging*

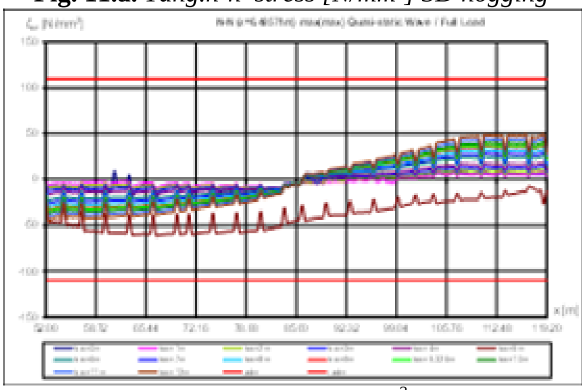

Fig. 11.b. *Tang.n-n stress [N/mm^2] 3D sagging*

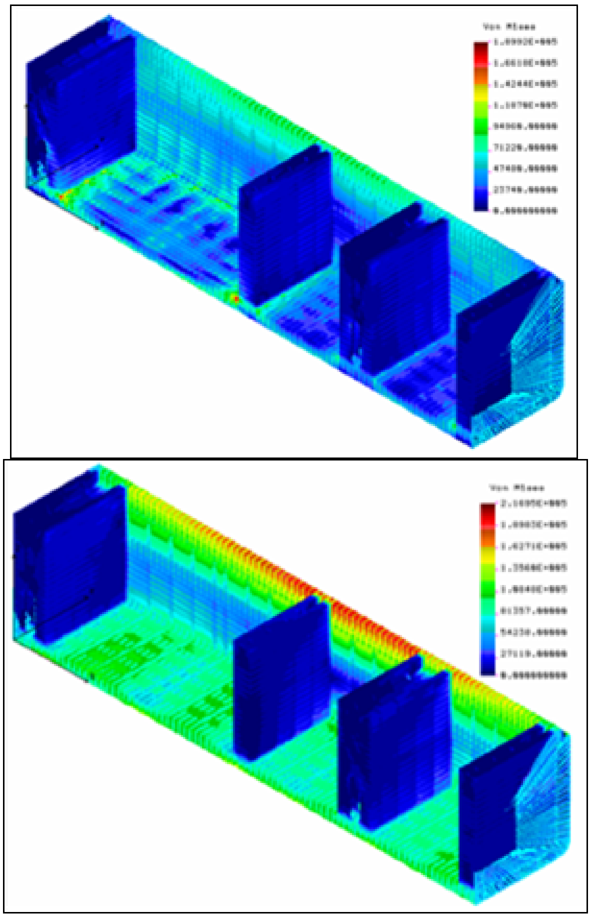

Fig. 12. *Von Mises stress 3D-FEM model hogg, sagg*

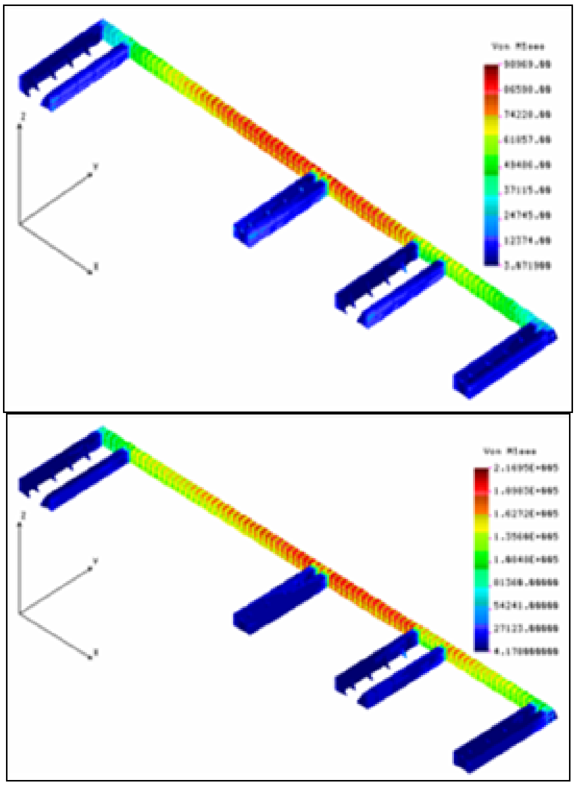

Fig. 13. *Von Mises stress Deck RL 3D-FEM hogg, sagg*

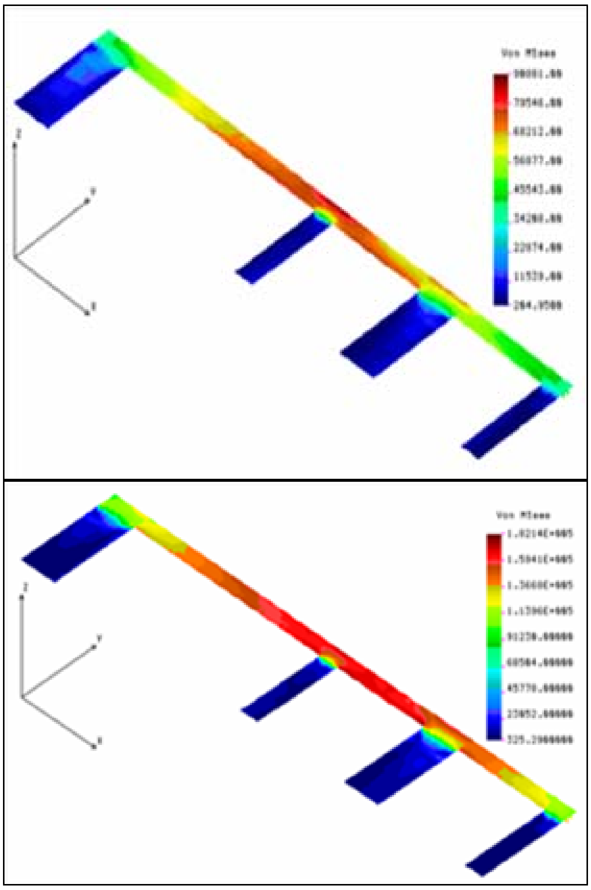

Fig. 14. *Von Mises stress Deck 3D-FEM hogg, sagg*

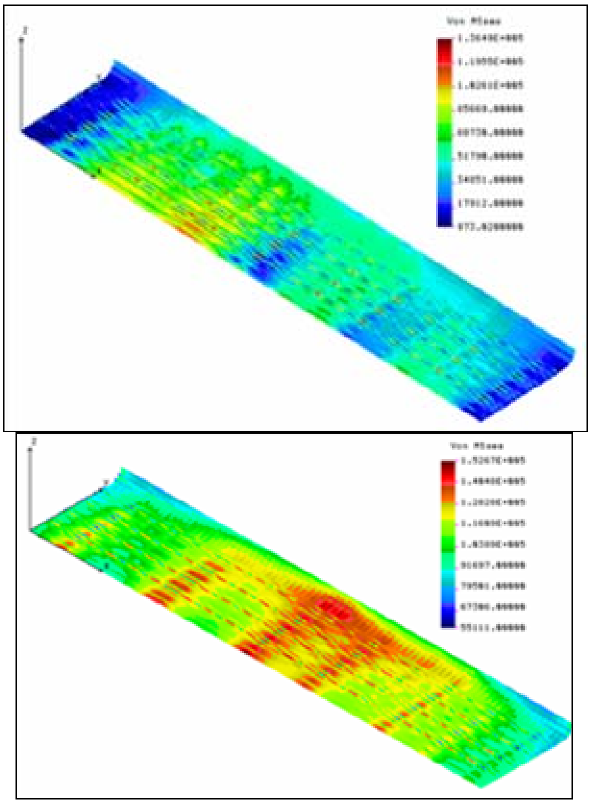

Fig. 15. *Von Mises stress Bottom 3D-FEM hogg, sagg*

4.2. Intermediary cargo case

In the following tables are included the next numerical results:

- the floating and trim in vertical plan equilibrium parameters, h_w, d_{aft}, d_{fore} , d_m, trim, for sagging and hogging cases (Table 8), intermediary cargo case.
- the maximum normal stress $\sigma_{x\text{-}max}$ [N/mm^2] using 3D-CAD/FEM and 1D-FEM models at sagging and hogging loading cases and their ratio, for deck RL and bottom (Table 9 and 10), intermediary cargo;
- the maximum tangential stress in the neutral axis, $\tau_{xz\text{-}max}$ [N/mm^2] using 3D-CAD/FEM and 1D-FEM models at sagging and hogging loading cases and their ratio (Table 11), intermediary cargo.

Table 8. *The floating and trim in vertical plan equilibrium parameters, intermediary cargo case*

h_w [m]	3D FEM Hogging			
	d_{aft}[m]	d_{fore}[m]	d_m [m]	trim [rad]
0	5.829	5.600	5.713	-0.00132
5	4.661	5.308	4.991	0.00373
9.326	3.268	5.188	4.249	0.01107
12	2.203	5.130	3.700	0.01688
	3D FEM Sagging			
0	5.829	5.600	5.713	-0.00132
5	6.103	6.387	6.244	0.00164
9.326	5.959	7.121	6.528	0.00670
12	5.866	7.468	6.642	0.00924

Table 9. *The maximum (max) normal stress, intermediary cargo case*

Hogging	$\sigma_{x\text{-}max}$ Deck RL [N/mm^2] (z=16m)		
h_w [m]	1D	3D-FEM	3D/1D
0	11.25	20.76	1.84
5	54.05	73.68	1.36
9.326	**87.36**	**101.8**	**1.16**
12	103.46	141.9	1.37
adm	224	224	
max_{GL}/adm	0.39	0.45	
Sagging	$\sigma_{x\text{-}max}$ Deck RL [N/mm^2] (z=16m)		
0	11.25	20.76	1.84
5	57.14	73.79	1.29
9.326	**119.28**	**224.40**	**1.88**
12	160.80	212.10	1.32
adm	224	224	
max_{GL}/adm	0.53	1.00	

Table 10. *The maximum (max) normal stress, intermediary cargo case*

Hogging	$\sigma_{x\text{-max}}$ Bottom [N/mm^2] (z=0)		
h_w [m]	1D	3D-FEM	3D/1D
0	9.13	33.92	3.72
5	36.85	73.68	2.00
9.326	**59.55**	**105.8**	**1.78**
12	70.53	122.00	1.73
adm	175	175	
$\max_{GL}$/adm	0.34	0.60	
Sagging	$\sigma_{x\text{-max}}$ Bottom [N/mm^2] (z=0)		
0	9.13	33.92	3.72
5	38.95	62.77	1.61
9.326	**81.31**	**122.9**	**1.51**
12	109.62	159.5	1.46
adm	175	175	
$\max_{GL}$/adm	0.46	0.70	

Table 11. *The maximum (max) n-n tangential stress, intermediary cargo case*

Hogging	$\tau_{xz\text{-max}}$ Neutral axis [N/mm^2]		
h_w [m]	1D	3D-FEM	3D/1D
0	18.36	9.39	0.51
5	33.95	19.13	0.56
9.326	**48.97**	**35.94**	**0.73**
12	56.89	36.56	0.64
adm	110	110	
$\max_{GL}$/adm	0.45	0.33	
Sagging	$\tau_{xz\text{-max}}$ Neutral axis [N/mm^2]		
0	18.36	9.39	0.51
5	34.14	12.9	0.38
9.326	**60.45**	**40.65**	**0.67**
12	78.19	39.27	0.50
adm	110	110	
$\max_{GL}$/adm	0.55	0.37	

In the following figures are presented the global-local strength numerical results, intermediary cargo:

- Fig.16 presents the mass diagram full cargo;
- the bending moment M [N/mm^2] diagram, based on 1D-girder model, for Deck RL (z=16m) and Bottom (z=0) wave height h_w=0-12m (Fig.17 and 18);
- the neutral axis normal stress τ_{xz} [N/mm^2] diagram, based on 1D-girder model, for wave height h_w=0-12m (Fig.19);

- the bending moment M [N/mm^2] diagram, based on 3D-CAD/FEM model, for Deck RL (z=16m) and Bottom (z=0) wave height h_w=0-12m (Fig.20 - 21);
- the neutral axis normal stress τ_{xz} [N/mm^2] diagram, based on 3D-CAD/FEM model, for wave height h_w=0-12m (Fig.22).

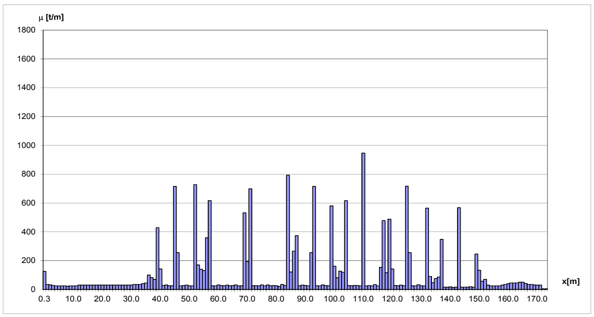

Fig. 16. *Mass distribution intermediary cargo*

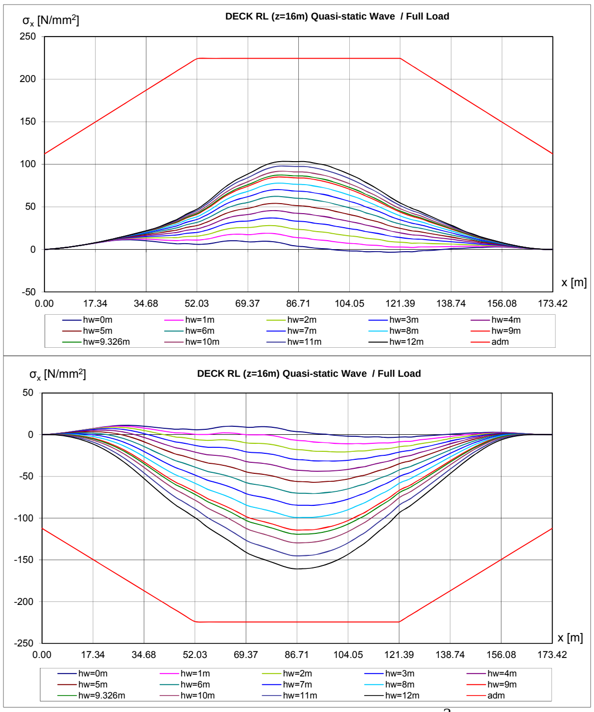

Fig. 17. *Normal stress Deck RL [N/mm^2] 1D hogg, sagg*

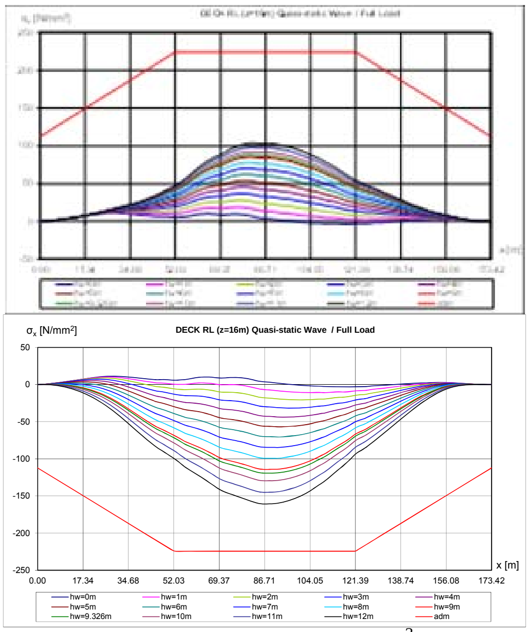

Fig. 18. *Normal stress Bottom [N/mm^2] 1D hogg, sagg*

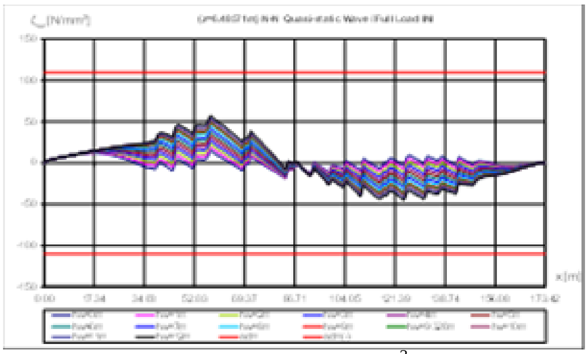

Fig. 19.a. *Tang.n-n stress [N/mm^2] 1D hogging*

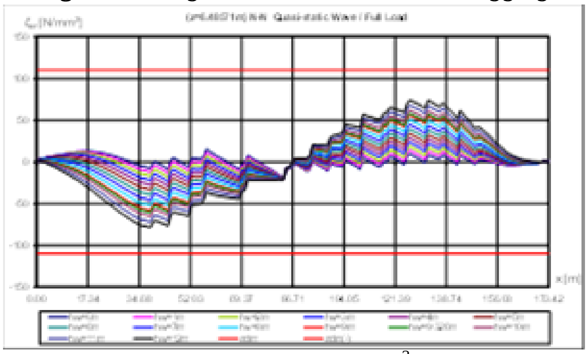

Fig. 19.b. *Tang.n-n stress [N/mm^2] 1D sagging*

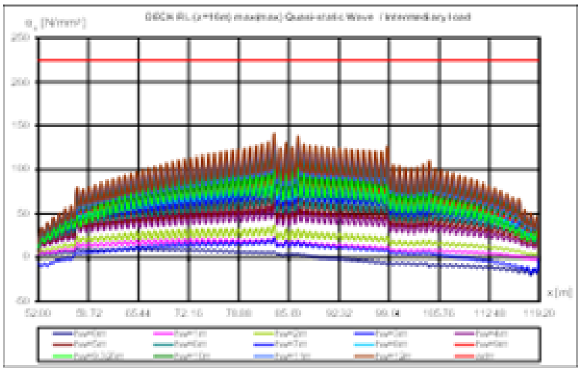

Fig. 20.a. *Normal stress Deck RL [N/mm^2] 3D, hogging (z=16m)*

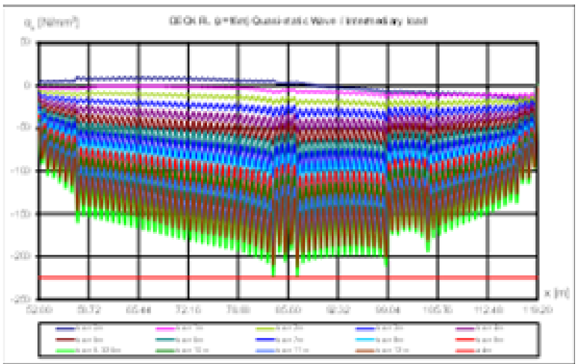

Fig. 20.b. *Normal stress Deck RL [N/mm^2] 3D sagging (z=16m)*

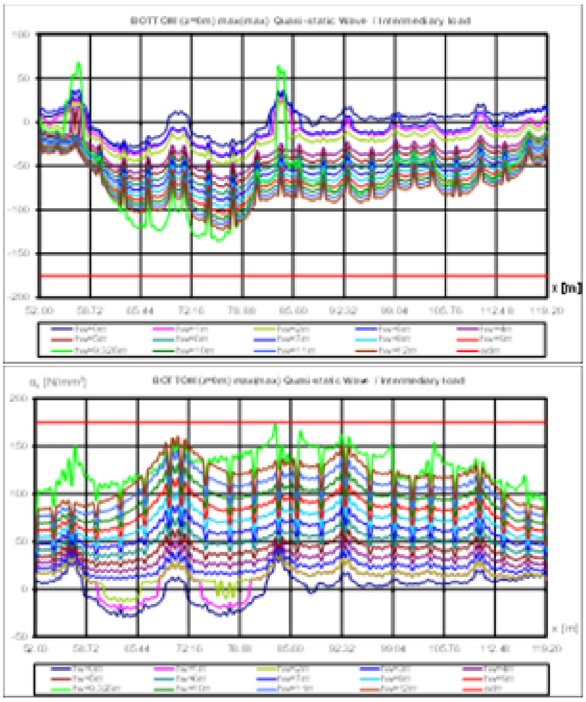

Fig. 21. *Normal stress Bottom [N/mm^2] 3D hogg, sagg*

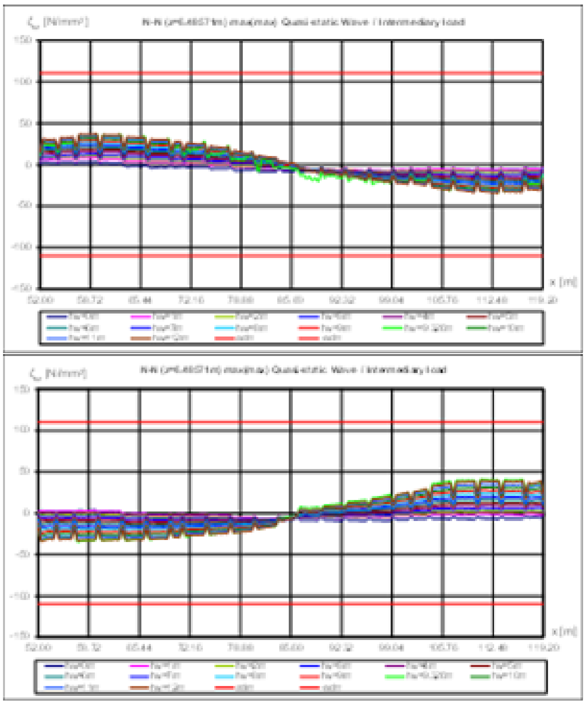

Fig. 22. *Tang.n-n stress [N/mm^2] 3D hogg, sagg*

In the following figures are presented the numerical results in the case of intermediary cargo:

- the equivalent von Mises stress [N/mm^2] distribution , at wave height h_w=9.326m, based on the 3D-FEM model, hogg and sagg case (Fig.23);
- the equivalent von Mises stress [N/mm^2] distribution for Deck RL (z=16m), Deck (z=14.5m) and

Bottom (z=0), at wave height h_w=9.326m, based on the 3D-FEM model, hogg and sagg case (Fig.24, 25 ,26).

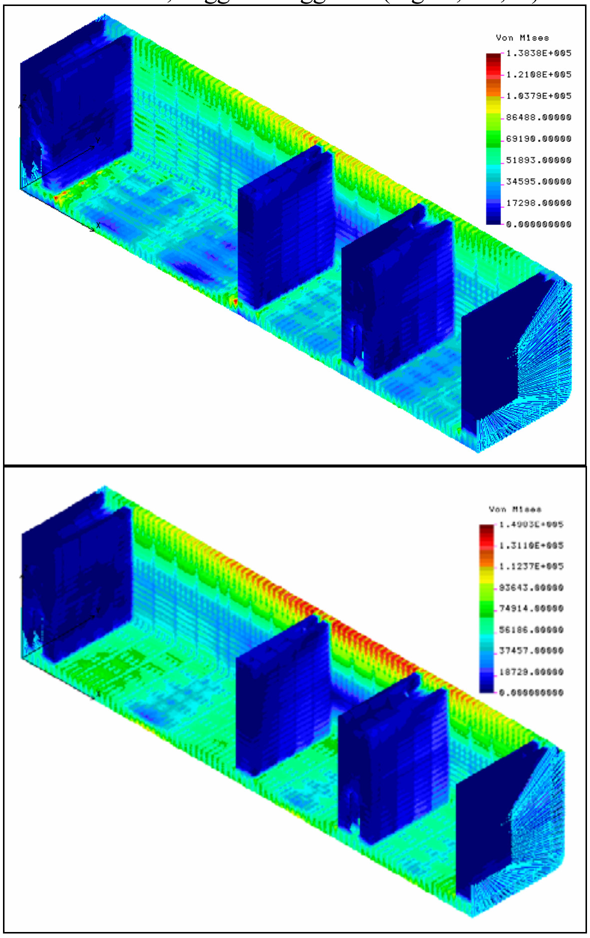

Fig. 23. *Von Mises stress 3D-FEM model hogg, sagg*

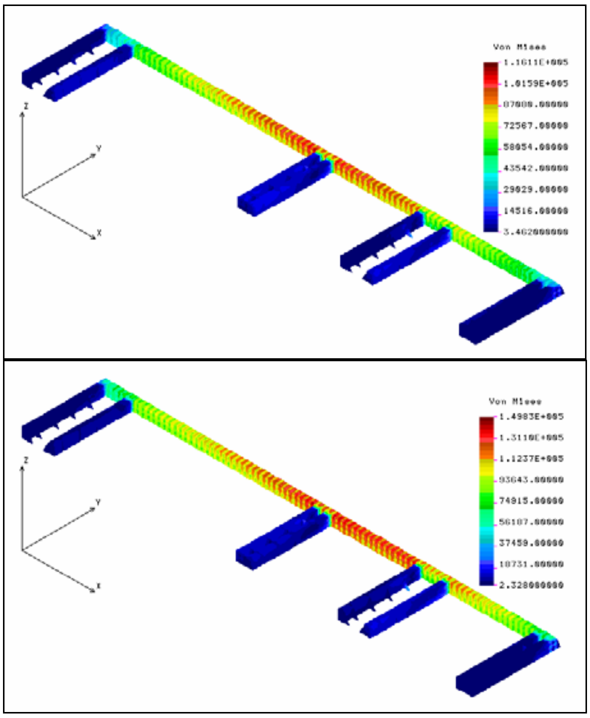

Fig. 24. *Von Mises stress Deck RL 3D-FEM hogg, sagg*

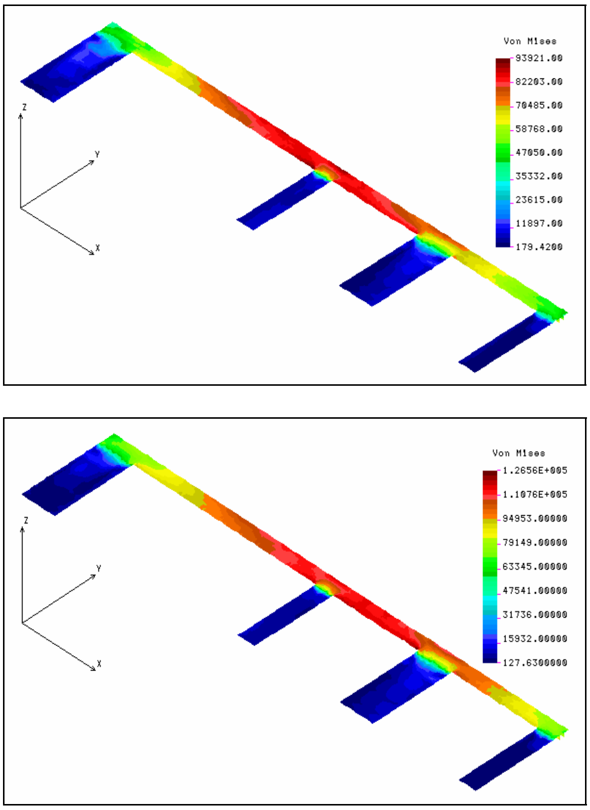

Fig. 25. *Von Mises stress Deck 3D-FEM hogg, sagg*

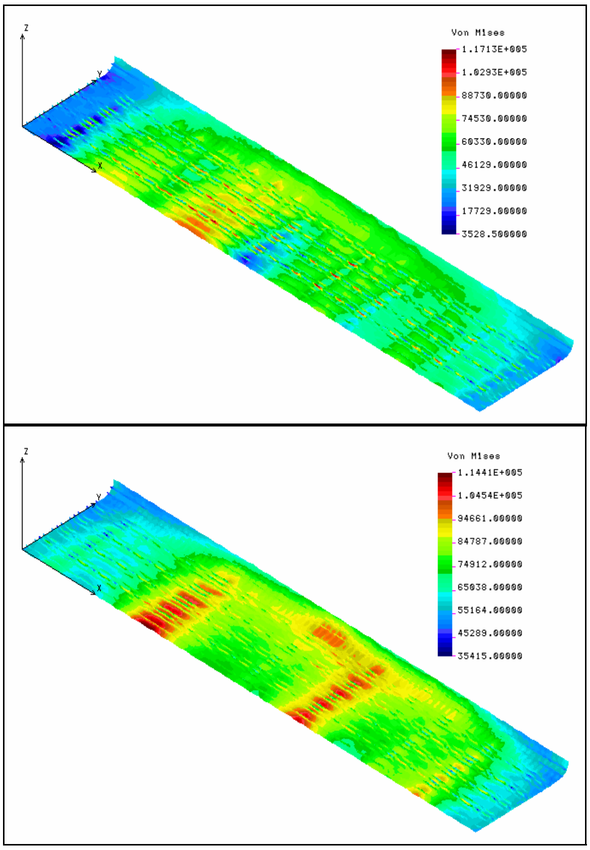

Fig. 26. *Von Mises stress Bottom 3D-FEM hogging and sagging*

5. CONCLUSIONS

Based on the numerical calculation from chapter 4, for the 1100 TEU container ship global-local strength analysis, the following conclusions can be drawn:

1. The maximum stress differences between 1D-girder models and 3D-FEM model, h_w=9.326m (Table 5) at full cargo case (containers on deck) for Deck-RL (z=16m) hogging condition are 1.31 times higher and for sagging conditions are 1.29 times higher; in the bottom (z=0) the stress difference (Table 6) in hogging conditions are 2.26 and for sagging are 1.33 times higher and in neutral axis the stress difference (Table 7) in hogging conditions are 0.61 and in sagging are 0.42 times higher.
2. At intermediary cargo case (no containers on deck) the stress differences are 1.16 for hogging and 1.88 for sagging Deck-RL (z=16m) (Table 9); in bottom (Table 10) for hogging 1.78 and for sagging 1.51 times higher and for tangential neutral axis (Table 11) the stress differences are 0.73 times higher for hogging and 0.67 times higher for sagging.
3. The maximum admissible stress values are not exceeded by the values obtained for both cargo cases. The stress ratio is $\sigma,\tau_{max}/\sigma,\tau_{adm} = 0.30 \div 1.01$, for the statistical wave height h_w=9.326 m.
4. The 3D-CAD/FEM model used for the global-local analysis makes possible to determine the global loads and to find the structures hot spot areas, which cannot be determined by 1D-FEM model.
5. In conclusion, the 1100 TEU container ship, under equivalent quasi-static head wave external load, satisfies strength in the central part cargo holds according to the Germanischer Lloyd Rules [4].

Acknowledgements

This study has been accomplished in the frame of the national grants TOP ACADEMIC POSDRU 107/1.5/S ID-76822 2011-2012 and EFICIENT POSDRU 88/1.5/S ID-61445 2011-2012.

REFERENCES

[1] Bathe, K.J., *Finite Elementen Methoden,* Springer Verlag [Book], 1990, Berlin;

[2] Domnisoru, L., *The finite element method applied in shipbuilding*, 2001, The Technical Publishing House, [Book], Bucharest;

[3] Domnisoru, L., Domnisoru, D., *The analysis of stress distribution in round or broken line form bracket flanges of ship structural joints"*, International Shipbuilding Progress Delft, No. 49(3), 2002, pp. 215-229;

[4] GL., "*Germanischer Lloyd's Rules"*, 2011, Hamburg;

[5] Frieze, P.A., Shenoi, R.A., (editors), *Proceeding of the 16th international ship and offshore structures congress (ISSC),* 2006, *Volumes 1 and 2*, University of Southampton;

[6] Lehmann, E., "*Guidelines for strength analyses of ship structures with the finite element method"*, 1998, Germanischer Lloyd Register, Hamburg;

[7] Servis, D., Voudouris, G., Samuelides, M., Papanikolaou, A., *Finite element modelling and strength analysis of hold no.1 of bulk carriers*, Marine Structures, No.16, 2003, pp. 601-626;

[8] Eyres, D.J., *Ship construction***,** *Boston* [Book], 2006, Butterworth Heinemann;

[9] Hughes, O.F., *Ship structural design. A rationally based, computer-aided optimization approach*, 1988, The society of naval architects and marine engineering, New Jersey;

[10] Ioan, A., Popovici, O., Domnisoru, L., *Global ship strength analysis*, 1998, Evrika Publishing House, Braila [Book];

[11] Rozbicki, M., Purnendu, K. Das, Crow, A., *The preliminary finite element modelling of a full ship*, International Shipbuilding Progress Delft, No. 48(2), 2001, pp.213-225.